

This is a repository copy of *Self-assembling, macroscopically oriented, polymer filaments; a doubly nematic organogel*.

White Rose Research Online URL for this paper:

<https://eprints.whiterose.ac.uk/138545/>

Version: Accepted Version

Article:

Gleeson, Helen F., Kaur, Sarabjot, Srigengan, Shajeth et al. (4 more authors) (2018) Self-assembling, macroscopically oriented, polymer filaments; a doubly nematic organogel. *Soft Matter*. ISSN 1744-683X

<https://doi.org/10.1039/C8SM01638K>

Reuse

Items deposited in White Rose Research Online are protected by copyright, with all rights reserved unless indicated otherwise. They may be downloaded and/or printed for private study, or other acts as permitted by national copyright laws. The publisher or other rights holders may allow further reproduction and re-use of the full text version. This is indicated by the licence information on the White Rose Research Online record for the item.

Takedown

If you consider content in White Rose Research Online to be in breach of UK law, please notify us by emailing eprints@whiterose.ac.uk including the URL of the record and the reason for the withdrawal request.



Journal Name

ARTICLE

Self-assembling, macroscopically oriented, polymer filaments; a doubly nematic organogel

Received 00th January 20xx,
Accepted 00th January 20xx

DOI: 10.1039/x0xx00000x

www.rsc.org/

Helen F Gleeson,^{*a} Harry Liu,^b Sarabjot Kaur,^{a,c} Shajeth Srigengan,^a V. Görtz,^d Richard Mandle^e and John E Lydon^f

Nanoscale phase separation and self-organisation in liquid crystals leads to the formation of remarkable hierarchical structures. There are several examples of heliconical nanofilament structures including in the nematic twist-bend (N_{TB}) phase, the B4 phase and liquid crystal gels formed from the B4 phase. Both the formation of the polymer-like structures that permeate the soft-solids and their hierarchical structures are fascinating, not least because of the analogies that can be drawn with naturally-occurring structures. Here, we report a remarkably simple binary system formed from a non-symmetric BC molecule and the rod-like liquid crystal, 5CB. The pure bent-core system exhibits both nematic and dark conglomerate liquid crystal phases. At very low concentrations of the BC material (5-10%) this binary system spontaneously self-assembles into a soft solid formed from nanoscale filaments that are aligned by their nematic environment. Macroscopically, the soft solid shows behaviour that can be associated with both polymers and gels. Interestingly, the sub-micron scale structure of the filaments appears remarkably similar to some organised fibrous structures in nature (e.g. chitin, cellulose, insect cuticle, plant cell walls) something we attribute to self-assembly and self-organisation in an aligned liquid crystalline environment. The nanoscale structure of the filaments show no features that can be associated with heliconical ordering down to length scales of tens of nanometers. However, the x-ray data suggests that a metastable rectangular columnar phase which is highly ordered in one dimension initially forms, changing to a hexagonal lattice on a timescale of tens of minutes.

Introduction

Hierarchical structures resulting from phase segregation of liquid crystalline (LC) physical gels are exciting systems because of the order that can appear on multiple length scales. Several levels of liquid crystal self-assembly into gel-like structures that exhibit switchable electro- and photo-switchable properties have been reviewed by Kato^{1, 2}. Most LC chemical gels (most commonly referred to as polymer-stabilised systems) contain less than 10% by weight of fibres that are polymerised. Reactive mesogens form a stabilising polymer network and the approach is commonly used to improve mechanical strength (shock resistance) and the electro-optic properties in liquid crystal devices. Another interesting class of liquid crystal chemical gels is produced by bent-core (BC) liquid crystals that exhibit the B4 phase. For

example, Zep *et al* describe a BC liquid crystal gelator that exhibits the B4 phase in bulk; various organic solvents were used to form the gels, though polar solvents did not show gelation³. The bulk B4 phase is known to form helical nanofilaments and similar structures were observed in the gels⁴. Zep *et al* note that in some cases nanotubules can form, stabilised in solution because the edge exposed to the solvent is much smaller than for twisted ribbons, reducing the energy cost. Kim *et al* report the growth of single helical nanofilaments from a 50:50 mixture of a BC material with the low molar mass mesogen 5CB (4-n-pentyl-4'-cyanobiphenyl) in the nanopores of an anodic aluminium oxide membrane⁵. There, the filament growth depends on the mixture parameters and nanopore dimensions. In that and related studies⁶, the underlying structure of the nanofilaments is again reminiscent of the B4 phase exhibited by the BC liquid crystal. Takanishi *et al* report helical nanofilaments formed in mixtures of a BC material in 5CB where there is a characteristic signature of the B4 phase⁷. The system we describe here does not require the B4 phase and shows a completely new kind of filamentary structure that permeates the nematic phase, resulting in a gel-like soft solid.

^a School of Physics and Astronomy, University of Leeds, Leeds LS2 9JT, UK.

^b School of Physics and Astronomy, University of Manchester, Manchester M13 9PL, UK.

^c Merck Chemicals Ltd., Chilworth, Southampton, UK.

^d Department of Chemistry, University of Lancaster, Lancaster, UK

^e Department of Chemistry, University of York, York UK

^f Faculty of Biological Sciences, University of Leeds, Leeds LS2 9JT, UK

† h.f.gleeson@leeds.ac.uk, author for correspondence.

Viscoelastic phase separation has recently been shown to cause the spontaneous formation of cellular structures in a bent-core/rod mixture⁸. The BC material used in that case, denoted BC20, exhibits a B7 phase and belongs to the homologous series of 4-n-octyloxyphenyl-3'-(2-fluoro-4-(3-fluoro-4-n-alkoxy-benzoyloxy) benzoyloxy)biphenyl-4-carboxylates. The striking resemblance to cellular structures that form in biological systems is noted by Pratibha *et al.*,⁸ who find that the morphology and stability of the structure is dictated by the relative concentration and orientation of the BC and rod-like molecule – in their case 8OCB (4-n-octyloxy 4'-cyanobiphenyl). The driving force of the phase separation is attributed to the much slower dynamics of the minority BC material compared with that of the majority phase.

The formation of filaments in pure bent-core liquid crystal materials is also extensively studied. As already mentioned, B4 filaments are well-known and filaments that form in the nematic phase of several oxadiazole materials have also been reported⁹. The nanoscale self-assembly in these cases is similar to that seen in the twist-bend nematic phase (N_{TB}), though filaments do not form in the N_{TB} phase^{10, 11}. Clearly, rich and interesting self-assembled nanostructures are being discovered in BC materials and their mixtures. This paper describes a novel binary system that includes very small quantities of a BC material, an oxadiazole material known as C5-Ph-ODBO-Ph-OC12 that exhibits both a nematic and dark conglomerate (DC) phase, dissolved in the rod-like material 5CB. The nanofibres that form in the system self-assemble in a direction controlled by the nematic director, with an 'interwoven' structure revealed by SEM that shows a striking resemblance to some biological systems, in this case biomechanical structures sometimes generally referred to as 'biological plywood'. We investigate the physical properties and nanostructure of the system and conclude that it is a nematic organogel, doubly nematic because the binary components and the final system are both nematic.

Methods and materials

Phase characterisation. The BC material, C5-Ph-ODBP-Ph-OC12, that self-organises into filaments in 5CB is an asymmetric oxadiazole-based material that has shown many interesting properties in both its nematic and DC phase¹². The structures and phase sequences of C5-Ph-ODBP-Ph-OC12 and 5CB are shown in Fig. 1. We describe in detail the results for a mixture containing 10 wt% of the BC compound, but note that the filaments were seen in other systems including in mixtures with as little as 5 wt% BC material in 5CB and at similar concentrations of other rod-like nematics, including 8CB. The formation of the filaments and the properties of the mixtures were studied using a variety of techniques that allow a detailed understanding of the filament structure and the behaviour of the soft solid. For polarizing optical microscopy

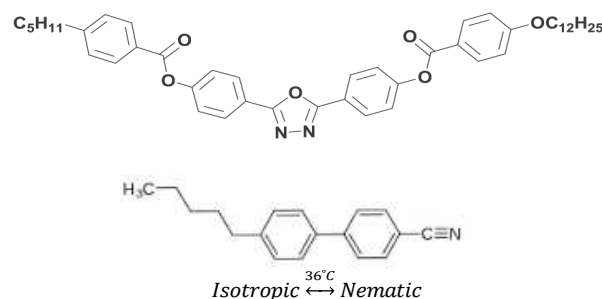
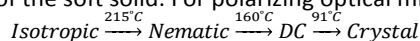


Fig. 1 The molecular structure and phase transitions of the pure bent-core oxadiazole compound C5-Ph-ODBP-Ph-OC12 (top) and the calamitic compound 5CB (bottom)/

and dielectric studies, devices of nominal thickness of $5\mu\text{m}$ were used with specific surface treatments to control the nematic director orientation. The sample temperatures were maintained with a relative accuracy of $\pm 0.1^{\circ}\text{C}$ for all experiments. A Mettler Toledo Differential Scanning Calorimeter (DSC) was used to confirm phase transitions that could be observed optically as well as to investigate the nature of the phase transition associated with the filament formation.

X-ray scattering. Small Angle X-ray Scattering (SAXS) was conducted using a bulk (unaligned) sample at the ESRF synchrotron, Grenoble, France. The X-ray energy was 12 KeV making the experiment sensitive to features from 1.5 nm to 9 nm and beam dimensions were of $0.2 \times 0.2 \text{ mm}$. The SAXS patterns were obtained using exposure times of typically 3 seconds; the experimental conditions were chosen as smectic-like structures are readily revealed in such circumstances, while allowing detailed experiments with various heating and cooling cycles.

Rheology. Rheology was carried out using an Anton Paar MCR 302 Modular Compact Rheometer. 25 mm diameter plates were used for the measurement and the distance between them was maintained at 0.75 mm. The measurement method was verified for pure 5CB at various temperatures (25, 30, 35, 38, 40, 45°C) under different strains. The relatively high viscosity of the BC/5CB mixture led us to employ an oscillatory rather than rotational mode. The storage and loss modulus together with the complex viscosity were measured from 25°C to 95°C at several angular frequencies.

Electron microscopy. SEM was carried out to observe the morphology of the sample using a FEI Quanta 200F (Field Emission Gun (FEG)-Environmental Scanning Electron Microscope (ESEM)). To carry out the SEM, the liquid crystal cell was carefully opened to expose the polymer structure. One of the plates was coated with a thin (5 nm) layer of platinum using a Cressington Sputter coater 208 HR (mtm 20). The conducting glass plate was mounted onto aluminium pin stubs with carbon adhesive tabs and carbon cement at the sample edges. The sample was placed in a horizontal field width and under high vacuum inside the SEM chamber. A

secondary electron detector (ETD) was used to obtain the highest magnification images.

The phase behaviour of the 10 wt% mixture

The phase behaviour of this and other filament-forming binary mixtures shows complex dependence on time and temperature. In general, a filament phase is observed in addition to the nematic phase. Fig. 2 shows the optical polarising microscopy images of the 10% BC mixture at various temperatures during heating and cooling cycles. Fig. 2(a) shows the network of filaments at room temperature within a nematic (N) background; we denote this a nematic+filament (N+F) phase. Upon heating to around 38°C the background nematic material undergoes a phase transition to the isotropic phase while the filament structure remains unchanged, Fig. 2(b). This background nematic to isotropic phase transition occurs at a slightly higher temperature than that of pure 5CB (~34°C) because of the dissolved bent-core material. Upon further heating, the filament structure is retained with an isotropic background (an I+F phase), melting completely to the isotropic (I) phase over the range 66°C – 72°C, Fig. 2(c).

The behaviour on cooling is quite different. The filaments do not form in the isotropic phase and instead the mixture cools from the isotropic phase directly into a nematic phase at a much higher temperature (~50°C) than the transition observed on heating. The filaments begin to form as soon as the nematic phase appears (50.3°C), Fig. 2(d), with a growth that is both time- and temperature-dependent. Fig. 2(e) shows the appearance of the N+F phase after the filaments completely dominate the sample at room temperature. The difference between the textures in Figs. 2(a) and (e) is attributed to the different cooling rates in each case, quenching from the isotropic phase and cooling slowly at 2°C/min respectively. Similar behaviour is observed in devices with homeotropic alignment; Fig. 3(a) is quench-cooled, while Fig. 3(b) is cooled at 2°C/min. When the mixture is cooled slowly, the filament growth is more readily aligned by the nematic director

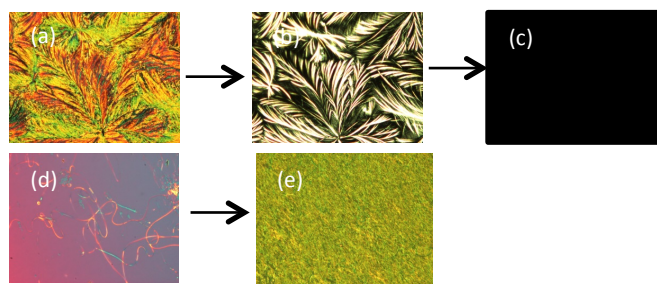
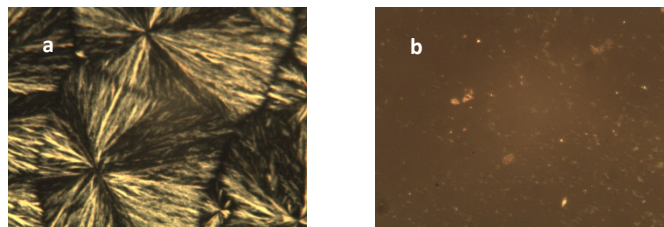


Fig. 2 Photomicrographs of planar samples at 100x magnification. (a) The N+F phase at room temperature. (b) I+F phase at 50°C (c) A pure isotropic phase at 80°C (d) The N+F phase 50.3°C in which the filament growth has just started, observed on cooling, (e) The N+F phase with filaments covering



the complete sample. Videos of this process, together with all of the data from this paper are <https://doi.org/10.5518/424>.

Fig. 3 Photomicrographs of homeotropic alignment. (a) The mixture quenched from the isotropic phase; the filaments have clearly nucleated and grown from specific points in the sample. (b) The mixture cooled at 2°C/min from the isotropic phase. At this slow cooling rate, the filament growth, guided by the homeotropic director, is in the perpendicular direction causing them to be less visible.

The phase transition temperatures observed depend on the sample history. On heating a sample with a well-established filament structure, the transition from the N+F to I+F phase is found to occur at 37.7°C. However, on heating a sample after the system has been cooled from the isotropic phase and allowed to stay at room temperature for a short time, the N+F to I+F phase transition is higher, 42.8°C. It takes around 24 hours at room temperature for the mixture to revert completely to its initial state. This observation suggests that the filaments are mainly composed of the bent-core dopant; the 'host' nematic structure has a transition closer to that of pure 5CB when the filaments have been forming for some time, whereas a system that has just cooled from the isotropic phase retains a large amount of bent-core component within the nematic phase, hence the higher nematic clearing point. Most interestingly, it seems that the nematic phase is critical to the formation of the filament phase in this system; the filaments do not form in the isotropic phase though they are retained in it once grown.

DSC measurements confirm the optical microscopy observations and additionally reveal further details of the phase behaviour of the system. Fig. 4(a) shows two runs carried out at a rate of 2°C/min; the initial cycle (run 1, black line) and a subsequent cycle (run 2, red line). Run 1 gives an onset temperature of 37.2°C for the N+F to I+F transition on heating, and 52.2°C as the I to N+F transition on cooling. Run 2 shows the N+F to I+F transition at an onset temperature of 41.1°C with 51.7°C as the I to N+F transition temperature while cooling. Fig. 4(a) additionally reveals a feature near 65°C associated with the melting of the filaments, observed optically between 65.7°C and 72.2°C. This peak does not change significantly between runs 1 and 2. However, it becomes much more prominent if the heating rate is increased to 20°C/min, Fig. 4(b). Such sensitivity to the heating rate is a feature of dynamic phase transitions, such as gel transitions, reinforcing our suggestion that the mixture forms a gel or gel-like system.

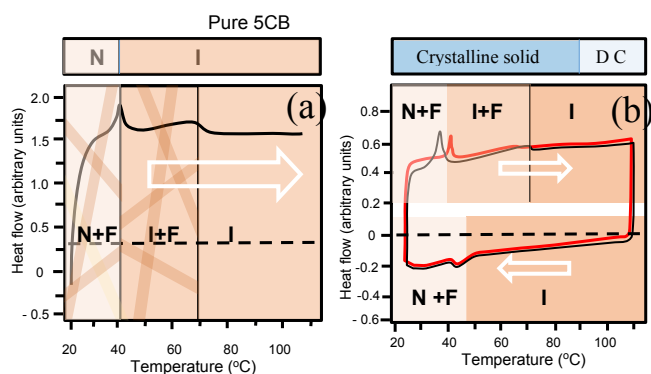


Fig. 4. The DSC traces which are compatible with the optical microscopy observations. (a) shows the DSC trace for a heating rate of 20°C/min. The curve has an endotherm at ~40°C, close to the clearing point of pure 5CB. The shaded areas in the rectangle above the graph indicate the temperature ranges over which pure 5CB is in the N and I states. (b) shows two heating and cooling cycles carried out at 2°C/min. The rectangle above the graph indicates the temperature ranges where the pure bent core compound is in the crystalline solid and the dark conglomerate states. The traces for the first and second cycles are black and red respectively. The two traces overlap for much of the cycle and are slightly offset for clarity. Note that there is no I + F phase observed on cooling. The thermal event that occurs on heating at 65°C corresponds to the temperature of melting of the filaments observed optically. This is a considerable distance from the solid to DC transition of the pure bent core material (shown above the graph). The position of the filament melting peak does not change significantly in position between runs 1 and 2. However, it is less prominent than that shown in (a) for the faster heating rate (b).

Analysis of the structure

A vial of the N+F phase at room temperature can be seen in Fig. 5, demonstrating that it can hold its own weight, a property shared with gels and polymers. The material is soft and malleable, does not flow, and yet has the appearance of a fluid nematic background when observed via polarizing microscopy. The birefringence colour of the nematic background changes with temperature, confirming that its nematic nature is retained. This system is quite distinct from other gel-forming liquid crystals discussed in the introduction, not least because it forms from two liquid crystalline molecules (differing from the gels formed by the B4-related materials) and there is no chemical reaction (thus distinct from polymer stabilised systems). A deeper insight into the structure of this soft-solid can be gained via rheology, x-ray scattering, and SEM experiments.

Fig. 6 shows the rheological properties of the mixture as a function of temperature in the N+F and I+F phases. The storage modulus G' exhibits a high value of $3.08 \times 10^5 \text{ Pa}$ at 25°C which reduces to a mere 2102.3 Pa at 65°C, the temperature where the filaments melt. The loss modulus in the same temperature region is lower than the storage



Fig. 5. The mixture contained in a vial at room temperature in both an upright and inverted position.

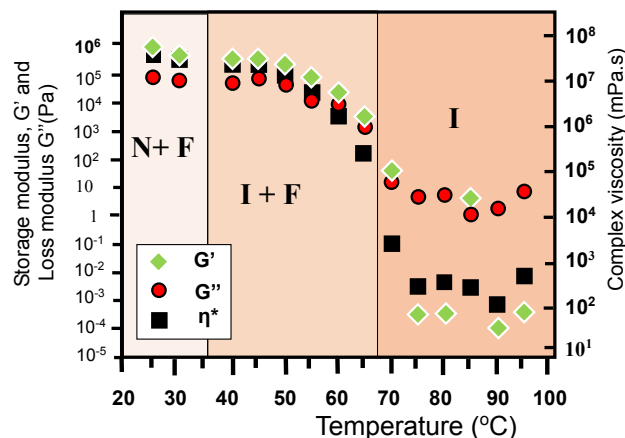


Fig. 6. The moduli and complex viscosity as a function of temperature determined at an angular frequency of 10 rads/sec.

modulus signifying that the material is a gel-like material. The loss modulus becomes more than the storage modulus at 75°C when the filaments melt which signifies liquid-like character of the material. The complex viscosity also follows the storage and loss modulus curve and exhibits an extremely large value of $3.12 \times 10^7 \text{ mPa.s}$ at 25°C which reduces to just less than 300 mPa.s at 75°C when the filaments have almost melted. For comparison, the viscosity of pure 5CB is ~100 mPa.s. The measurements were carried out at a strain of 0.05%, which is in the linear region. Similar rheological behaviour is found for other polymer systems such as PDMS, polystyrol etc.^{13, 14} The storage and loss moduli in our system resemble organogels which also exhibit G of the order of 10^5 Pa . Despite the very different chemistry in our mixtures from more traditional organogels, the rheological properties are strikingly similar.¹⁵

SAXS measurements were undertaken to probe the molecular organisation in the system. Fig. 7 (top) shows a typical x-ray diffraction pattern from a bulk sample held in a Kapton packet (the Kapton is responsible for the diffuse outer diffraction ring). The peaks of interest are marked A and B and both are associated with the filament structure. The narrow full-width half maximum of peak B indicates a well-defined periodic structure whilst peak A is significantly more diffuse,

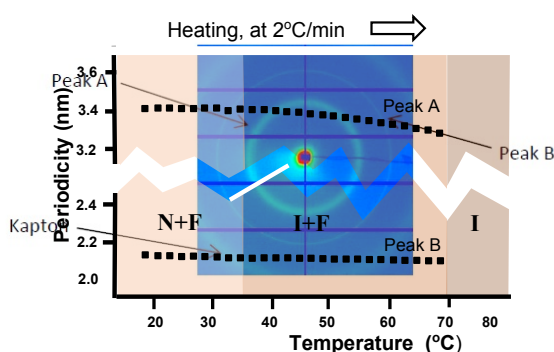


Fig. 7. (top) The X-ray diffraction pattern of a bulk sample of the mixture held at room temperature for more than 24 hours, and thus in the N+F phase. (bottom) The temperature dependence of positions of peaks A and B, determined on first heating of the sample from a well-established N+F phase. The transition from the N+F into the I+F phase occurs at $\sim 37^\circ\text{C}$.

reminiscent of the diffraction pattern from the dark conglomerate (DC) phase observed in the pure BC material¹⁶.

There is also significant scattering at very small angles close to the beam stop, the intensity of which decreases significantly as the sample is heated through the temperature range where the filaments are observed to melt. A small remnant of that very small-angle feature is retained much further into the isotropic phase, at temperatures as high as 100°C , with a scattering intensity much less than 25% of that in the phases where the filaments are clearly visible. This feature of the SAXS pattern at very small angles can be attributed to a polymer-like structure, but the camera length, optimised for length scales of $\sim 3\text{ nm}$, did not allow detailed studies of the polymer-like structure.

The behaviour of peaks A and B on heating at ($2^\circ\text{C}/\text{min}$) is shown in Fig. 7 (bottom). Both disappear at the I+F to I phase transition, with little change in position of either as a function of temperature. A small, but significant change in the periodicity of A is observed on increasing temperature, varying from 3.43 nm at room temperature to 3.30 nm just below the transition to the isotropic phase. The periodicity of B remains approximately constant throughout (2.17 nm at room temperature and 2.14 nm at the phase transition). Interestingly, a periodicity of 3.4 nm is close to the molecular length calculated for one conformer of Compound 1 and is identical to the 3.4 nm periodicity measured at low temperatures in the DC phase of the material.^{9, 15, 16} The diffuse nature of peak A is also reminiscent of the scattering characteristic of the DC phase. The periodicity of peak B, $\sim 2.1\text{ nm}$, is much closer to that found for 5CB ($\sim 1.8\text{ nm}$), but not sufficiently close to offer a robust explanation for it.¹⁷ Despite the fact that the phase transition from N+F to I+F around $\sim 38^\circ\text{C}$ is clearly observable via polarizing microscopy and DSC, there is no change in the SAXS pattern until the mixture becomes completely isotropic.

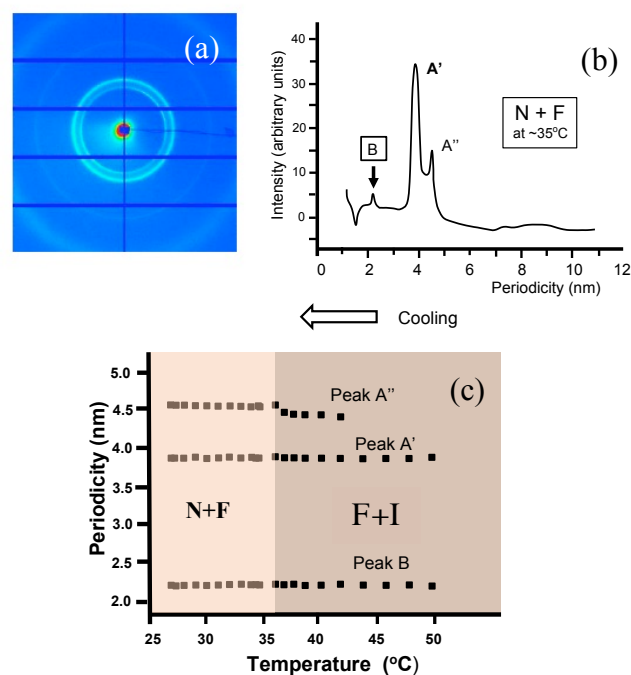


Fig. 8. (a) The SAXS pattern obtained immediately following cooling into the N+F phase at $2^\circ\text{C}/\text{min}$ from the isotropic phase. (b) The integrated intensity from the SAXS pattern of a sample at 35°C , immediately after cooling into the N+F phase (from just above the N+F to I+F transition temperature). Note the position of the relatively invariant peak B (at 22 nm) and the fully-resolved A' and A'' peaks. The split peak is now denoted A' and A''. (c) The positions of peaks A', A'', and B as a function of temperature on cooling from just above the F+I transition. Although no filaments are observed optically under similar circumstances, the peaks were clearly visible provided that the cooling cycle occurs immediately, and can be attributed to assembly of the polymer-like structure that remains up to much higher temperature.

Upon cooling at $2^\circ\text{C}/\text{min}$, the SAXS data exhibit some very interesting behaviour. On cooling into the N+F phase, peak A exhibits two clear components, while peak B remains unchanged, Fig. 8(a). Integration of the intensity of SAXS pattern results in the data of Fig. 8(b), showing the two distinct peaks, one close to $\sim 3.8\text{ nm}$ (denoted A') and the other at $\sim 4.5\text{ nm}$ (A''), both shifted significantly from the original peak A at $\sim 3.4\text{ nm}$. Peak B remains unchanged at $\sim 2.2\text{ nm}$. The temperature dependence of the features is shown in Fig. 8(c).

The periodicities measured in the mixture are rather difficult to understand in detail, but we note the following. Peaks A' (3.85 nm) and A'' (4.54 nm) are quite close to the values determined in the nematic phase of the pure bent-core compound ($\sim 4.3\text{ nm}$) and therefore must originate from the BC material. However, the occurrence of two distinct peaks is a surprise. Fig. 8c shows the temperature dependence of the periodicity of the peaks A', A'', and B on cooling from the isotropic phase; the experiment was performed immediately following the heating cycle to just above the I+F transition. Although peak A'' comes into existence at the same temperature as others (just into the I+F phase), the scattering

is too weak and diffuse to fully analyse and it only becomes distinct well into the N+F phase at 41.9°C and fully defined at 36.9°C. Peak B cannot readily be associated either with 5CB or with the BC compound alone. The fact that the peaks are observable at all temperatures in the I+F phase region, under circumstances where there is no optical evidence of the fibres, suggests that the polymer-like structure that is retained to temperatures much higher than the I+F transition begins to self-assemble immediately below the transition. Following this process is clearly of interest for the future.

It is clear that the formation of the filaments is occurring via self-assembly of both the BC molecule and 5CB in the background nematic phase and it is illustrative to consider similarities to filament formation in both the B₄ and the twist-bend (N_{TB}) nematic phases. Chen et al.¹⁰ describe the heliconical structure of the N_{TB} phase observed in several compounds in detail with the bent-core material, UD68 of particular relevance here. That material forms N, N_{TB} and rectangular columnar phases with nematic periodicity of ~3.1nm and rectangular lattice parameters of ~3.1nm and 2.2nm. The very diffuse nature of peaks A, together with the highly ordered peak B leads us to suggest that the filaments self-assemble with a structure that is initially columnar in nature, highly-ordered in one dimension. The other dimension evolves from two periodicities, with the diffuse nature attributed to frustration in the packing and low correlation lengths, as occurs in the DC phase.

The final aspect of the X-ray data to consider is time dependence of the evolution of peaks A, shown in Fig. 9. It can be seen that the two diffuse peaks A' and A'' observed on initial cooling rapidly converge into a single peak, A over a period of ~30 minutes. The position of this single peak continues to drift slowly with time, indicating a reduction in the repeat distance of the A spacing. The inference is that whilst filaments form immediately on cooling into the nematic phase, there is a rapid change in symmetry of the structure of the filaments, followed by a slow 'annealing' process, involving a minor adjustment of dimensions over a time scale of hours, before the final, stable, filament structure is established.

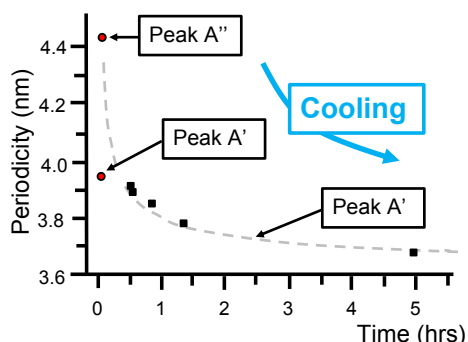


Fig. 9. The change in position of the peaks A, A' and A'' after cooling from the isotropic melt to room temperature. The two peaks A' and A'' observed initially, rapidly converge into a single peak, A over a period of ~30 minutes. The position of this single peak continues to drift slowly with time, indicating a reduction in the repeat distance of the A spacing. The inference is that whilst filaments form immediately on cooling into the nematic phase, there is a rapid change in symmetry of the structure of the filaments, followed by a slow 'annealing' process, involving a minor adjustment of dimensions over a time scale of hours, before the final, stable, filament structure is established.

timescale of ~30 minutes). The periodicity continues to change slowly with time, converging towards 3.4nm over ~24 hours. The thermal data make it clear that both the 5CB and the BC molecule are incorporated into the filament and that while filaments form immediately on cooling into the nematic phase, there is a refining process that occurs on a long timescale that results in the final, stable, filament structure. That structure includes the majority of the BC material; clear from the fact that the transition temperature of the background nematic phase becomes closer to that of pure 5CB as the filament structure stabilises.

Further detail is revealed on subsequent heating runs, Fig. 10. The difference in the initial heating and subsequent heating runs is attributed to the time dependence of the formation of the filaments. In systems where the filaments are not in their equilibrium structure (when they will exhibit peak A at 3.4nm), the periodicities displayed also differ, as shown in Fig. 10. The behaviour in the two subsequent heating runs depends on how long the sample has been allowed to develop the filament structure. The runs shown in Fig. 10 were under quite different conditions; in the first heat, the sample was held at each measurement temperature for several minutes, while for the second, a continuous heating rate of 2°/min was employed. The former case allows more time for the time-dependent system to adapt to the changing temperature. In both runs, there is a region of ~5K just below the isotropic phase transition where the periodic structure is stabilized with a

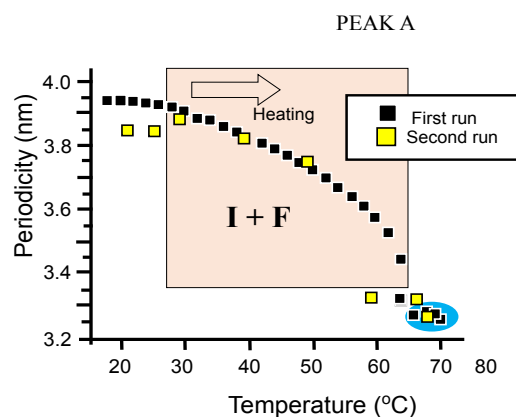


Fig. 10. The temperature dependence of peak A on sample history. For the first heating run, the sample was held at each measurement temperature for several minutes. For the second run, it was heated at a continuous rate of 2°C/min. We attribute the difference in values observed to the time required for the filaments to assemble on a nanoscale. In both runs, there is a region of ~5K just before the clearing point, where the filament structure is stabilised, with a periodicity of ~3.3nm. The shaded rectangle indicates the presumed boundaries of the I+F state. The diffraction patterns given by samples within the blue shaded oval appear to be identical to that of the dark conglomerate phase of the pure bent core compound.

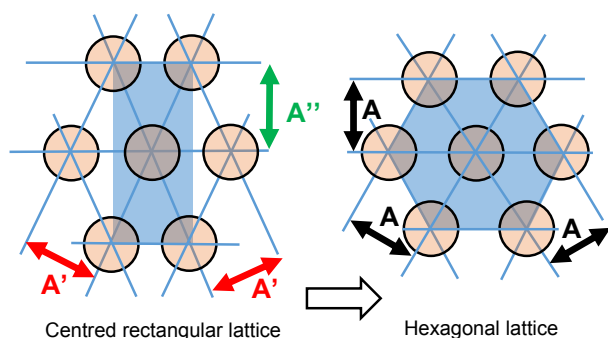


Fig. 11. The proposed change in symmetry of a two-dimensional lattice of columns which would explain the convergence of the A' and A'' spacings with increasing temperature or with time. In the metastable, centred rectangular cell the three principal spacings are the 1,1 and symmetry equivalent $\bar{1},1$ (repeat distances indicated by the red double-headed arrows) and the 2,0 spacing (green). In the hexagonal lattice all spacings are identical, giving the single A reflection.

periodicity around 3.3 nm . This stabilization in periodic structure appears to be a phase transition in the material and the x-ray pattern becomes broad and diffuse, similar to that observed in the DC phase of the pure material^{9,16}. The appearance of a DC phase would not be seen via polarizing microscopy as the phase is optically isotropic.

Bringing together all of the x-ray information, including the complex thermal behaviour leads us to suggest that the filaments self-assemble as a columnar structure, initially with a metastable centred rectangular cell and evolving with time into a hexagonal cell, figure 11. Such a change in symmetry explains the convergence of the A' and A'' peaks. Further, the fact that the A' peak in Figure 8b is approximately twice the height of A'' supports this model (as there are twice as many reflections corresponding to A' as to A'').

Scanning Electron Microscopy (SEM) was carried out to understand the structure of the gel phase formed. Fig. 12 shows SEM images of the 3-D network formed by the filament structure. The network obtained for the mixture shows some resemblance to other organogel networks imaged with SEM¹⁹, though in Ref. 19 the solvent was isotropic and clear 3-D isotropic networks are formed that are not obvious from our images. Rather, the filament network that is responsible for the macroscopic gel-like properties apparent from Fig. 5 has several distinctive features. Firstly, the filaments are highly orientated, a property that is also clear from the macroscopic polarising microscopy observations. Secondly, the interwoven nature of the structures can only occur because the filaments are self-assembling whilst growing at the ends. The third observation that one can make is that the fibre network is quite dense, despite the system only containing 10% w/w of the BC liquid crystal. Finally, at the highest magnification, where the filament bundle width is of the order of tens of nanometers, there is no indication of a helical structure,

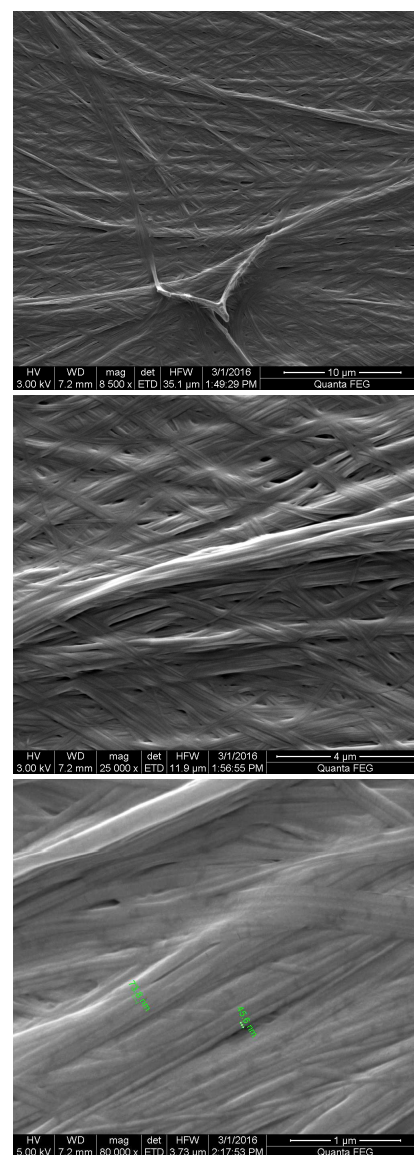


Fig. 12. SEM of the filament structure with increasing magnification. (top) The scale bar represents $10\mu\text{m}$ and it is clear that the filament structure is being controlled by the director orientation around the defect; (middle) The scale bar represents $4\mu\text{m}$ and an interesting 'woven' feature of the filaments is apparent; (lower) The highest magnification of the structure obtained (scale bar is $1\mu\text{m}$) and no helical features can be seen in the bundles which are several tens of nanometers in width.

though this would be clearly visible in images of similar magnification of the B4 phase. It is noteworthy that very similar structures to those seen in figure 12 are observed in 'nature's plywood' (cellulose, chitin, collagen, bone etc.).²⁰ Such ordered growth is of significant interest and we have identified two features of the system here that are implicit in the formation of this structure; a self-assembling process whereby filaments grow from their ends and directionality imposed by the nematic director. It is interesting to suggest that the same influences must be present in forming the naturally-occurring structures and that we have shown the

clear influence of the background nematic phase on the structure.

Discussion and Conclusions

There have been many studies of systems in which small amounts of a bent-core liquid crystal have been included in calamitic nematics, particularly in the early stages of understanding their anomalous elastic behaviour (see [12] and references therein). While many showed the expected suppression of the bend (k_{33}) elastic constant, none exhibited this unusual filament formation. The most similar occurrence, apart from filaments that form in very narrow temperature regimes of the nematic phase in some pure BC nematic materials⁷, is perhaps the cellular structure formation reported by Pratibha *et al*, but the concentrations of the BC material used here are 5-10%, much lower than the 10-30% concentrations of the BC20 material in ref 8. This system is therefore highly unusual and shows several interesting features. Indeed this particular BC material is also very unusual and has been the subject of several papers^{12, 21}.

What is particularly interesting about the mixed system is that irrespective of the pronounced hysteresis in this system, the filaments form only in the nematic phase. Further, they self-assemble in a direction that is controlled by the nematic director. The resulting soft solid has all the characteristics of a gel and can therefore be characterised as an organogel. The DSC results indicate that a small amount of the 5CB present is intimately associated with the BC molecules in the filaments and alters their pattern of aggregation. Once the filaments have formed, the fact that there is no further change in the transition temperatures indicates that a stable structure has been achieved in which only a small amount of BC material is still dissolved in the 5CB (a conclusion drawn from the slightly higher transition temperature of the nematic portion of the final mixture).

The filaments initially formed on cooling are in a metastable form with a structure related to, but not identical to the stable form to which the system gradually reverts. Indeed the evolution of the x-ray scattering peaks A' and A'' are associated with this evolution and we also observe that the transition from the A'+A'' state to peak A is weakly first order. The A' and A'' peaks are associated with a relatively highly ordered state with a lower symmetry (probably centred rectangular) than that where only peak A is observed (probably hexagonal). As peak B is unaffected by sample history or heating/cooling the sample, we suggest that this reflection is associated with the internal structure of the fibres while peaks A are all associated with columnar spacing.

This intriguing filament structure appears to be reliant on the BC material C5-Ph-ODBP-Ph-OC12; we have seen similar structures form in other calamitic host liquid crystal systems

with this BC material as a dopant, but not with other BC materials. This is an intriguing observation, but we note that C5-Ph-ODBP-Ph-OC12 has proven to be a most unusual BC liquid crystal in terms of its other physical properties and their behaviour with temperature. It is perhaps also noteworthy that this is one of the very few BC materials in which the DC phase is observed directly below the nematic phase and suggest that the similarity of the DC phase structure with aspects of the filament structure is implicit in the formation.

Finally, we emphasise that this organogel system is significantly different from most conventional gel networks formed. Firstly, both the filament network and the background phase are made from liquid crystalline materials, unlike other liquid crystal gel systems in which the liquid crystal forms only one component of the gel system. Further, this is a simple, two-component system with no chemical bonds formed between the components, again distinguishing it from many other kinds of gel. Finally, the filament network orientation is controlled by the nematic director whereas other gel networks are isotropic. Clearly, we have unusual self-assembly that forms a self-organised gel structure in a soft solid that combines three soft-matter material types; liquid crystals, polymers and gels. As the gel forms in the nematic phase, the network formation is oriented by the director and the continuous (liquid) phase in the gel remains nematic, the system is a doubly nematic organogel.

Conflicts of interest

There are no conflicts to declare.

Acknowledgements

The x-ray data in Figs. 7 and 8 were determined at the ESRF, Grenoble. Thanks are due to Wim Bras, Mamatha Nagaraj, Vitaly Panov and Cliff Jones for their contributions to the run during which these experiments were performed. HL is grateful to Merck Chemicals (Chilworth, UK) and the Engineering and Physical Sciences Research Council, UK for a CASE award that funded his studentship.

Notes and references

- 1 T. Kato, *Science*, 2002, **295** 2414
- 2 T. Kato, Y. Hirai, S. Nakaso and M. Moriyama, *Chem Soc Ref.*, 2007 **36**(12) 1845
- 3 A. Zep, M. Salamonczyk, N. Vaupotic, D. Pociecha and E. Gorecka, *Chem Comm.*, 2013 **49** 3119
- 4 J. Matraszek, N. Tobnani, N. Vaupotic, H. Takezoe, J. Mieczkowski, D. Pociecha and E. Gorecka, *Angewandte Chemie*, 2016 **55** 3468
- 5 H. Kim, S. H. Ryu, M. Tuchband, T. Joo Shin, E. Korblova, D. M. Walba, N. A. Clark, D. K. Yoon, *Science Advances* 2017 **3** e1602102
- 6 H. Kim, Y. Yi, D. Chen, E. Korblova, D.M. Walba, D.K. Yoon, *Soft Matter* 2013 **9**(10) 2793

- 7 Y. Takanishi, H. Yao, T. Fukasawa, K. Ema, Y. Ohtsuka, Y. Takahashi, J. Yamamoto, H. Takezoe and A. Iida, *J Phys Chem B*, 2014 **118** 3998
- 8 S. Anjali and R Pratibha, *Soft Matter*, 2017 **13** 2330
- 9 V. Gortz, C. Southern, N. W. Roberts, H. F. Gleeson and J. W. Goodby, *Soft Matter*, 2009 **5** 463
- 10 D. Chen, J. H. Porada, J. B. Hooper, A. Klittnick, Y. Shen, M. R. Tuchband, E. Korblova, D. Bedrov, D. M. Walba, M. A. Glaser, J. E. MacLennan and N. A. Clark, *Proc. Natl. Acad. Sci. U. S. A.*, 2013 **110** 15931
- 11 V. Borshch, Y. K. Kim, J. Xiang, M. Gao, A. Jakli, V. P. Panov, J. K. Vij, C. T. Imrie, M. G. Tamba, G. H. Mehl and O. D. Lavrentovich, *Nat. Commun.*, 2013 **4** 2635 DOI: 10.1038/ncomms363
- 12 S. Kaur, J. Addis, C. Greco, A. Ferrarini, V. Gortz, J. W. Goodby and H. F. Gleeson, *Phys. Rev. E*, 2012 **86** 041703
- 13 Y. Fan, S. Dai and R. I. Tanner, *Korea-Australia Rheology Journal*, 2003 **15** 109
- 14 D. P. Heberer, J. A. Odell and V. Percec, *J. Mater. Sci.*, 1994 **29** 3477
- 15 J. H. Lee, J. Park, J-W. Park, H-J. Ahn, J. Jaworski, H. H. Jung, *Nature Communications* 2014 DOI: 10.1038/ncomms7650
- 16 M. Nagaraj, K. Usami, Z. Zhang, V. Görtz J.W. Goodby & H.F. Gleeson, *Liquid Crystals*, 2014 **41** 800
- 17 M. Nagaraj, J. C. Jones, V. Panov, H. Liu, V. Görtz, J.W. Goodby and H.F. Gleeson, *Physical Review E* 2015 **91**(4) 042504
- 18 A. Leadbetter, R. Richardson and C. Colling, *le Journal de Physique Colloques*, 1975 **36(C1)** C1-37
- 19 X. Ran, L. Shi, K. Zhang, J. Lou, B. Liu and L. Guo, *Journal of Nanomaterials* 2015 357875
- 20 A. C. Neville, *The Biology of Fibrous Composites* 1993, Cambridge University Press.
- 21 S Kaur, V P Panov, C Greco, A Ferrarini, V Görtz, J W Goodby and H F Gleeson, *Appl. Phys. Letts.*, 2014 105223505